Digest Journal of Nanomaterials and Biostructures Vol. 19, No. 3, July -September 2024, p. 1199 - 1205

Polythiophene/graphene oxide thin films: optical properties

J. Martínez, F. Retana, I. Gómez*
University Autonomous of Nuevo Leon, Faculty of Chemical Sciences, Materials Laboratory I, Avenida Universidad, Ciudad Universitaria, 66455, San Nicolás de los Garza, N.L. Mexico.

Thin films of polythiophene/graphene oxide (PTh/GO) were prepared using chronoamperometry. X-ray diffraction (XRD), Fourier transform infrared spectroscopy (FTIR), scanning electron microscopy (FESEM), UV-Vis spectroscopy, and photoluminescence spectroscopy (PL) were used for characterization purposes. PTh and PTh/GO thin films were achieved through chronoamperometry at a constant anodic potential of +1.9 V vs. Ag/AgCl. The PTh/GO thin films exhibited visible light absorption. The thicknesses of the thin films were approximately 2.42 μm.

(Received June 5, 2024; Accepted August 5, 2024)

Keywords: Polythiophene, Graphene oxide, Thin films, Chronoamperometry

1. Introduction

The interest in polythiophene-based composites is based on their electrical conductivity, optical properties, thermal and chemical stability, and ability to create flexible devices. Polythiophene and its composites materials are now extensively researched for energy storage applications and electronic instruments, for example, batteries, fuel cells, light-emitting diodes (LEDs), supercapacitors, solar cells, anticorrosive coatings, sensors, etc. [1–4]. These polythiophene films can be prepared from the monomer by electrochemical or chemical polymerization techniques and demonstrate a range of electrical exploitable properties with also optical advantages related to this category of technology. In this regard, one important feature of the electrochemical method is that it allows for fabricating thin films with high quality film growth.

Highly conductive materials have a very strong appeal in the area of printed macroelectronics and other electronic devices. The intention behind this is to remove heavy metal-based current collectors with thin, flexible, light weight films which are highly conducting to further increase energy density of such devices. One possibility that appears quite attractive for film production is two-dimensionally shaped building units including graphene and reduced graphene oxide (rGO) nanosheets because are cheap and present a high aspect ratio, low percolation threshold and excellent flexibility. The focus on the development of graphene for flexible electronics has seen new applications like Cyberskin[5], wearable devices[6], and motion sensors[7]. However, graphene based materials are considered ideal candidates for electrically conducting components because they are bendable and flexible; nevertheless, the utilization of nanomaterials in electrochemical biosensors represents a novel approach towards electrochemical biosensor design [8–13].

Graphene oxide combined with polythiophene has been investigated for its synergistic potential due to the strong π-π* interactions that result from it between these materials leading to the creation of more ordered regions within composite enhancing overall performance. However, the use of these films in flexible optoelectronic devices and solar cells is still under investigation[14,15]. Several methods have been investigated to enhance the desired properties of different materials. Analyzing how various nanoparticles sizes, shapes, even used as decorations, being impactful in the composites performance is one of the most often used techniques [1–3,16].

An in-depth analysis of the main polymer synthesis methods showed that the chemical oxidative approach, despite its cost-effectiveness, faces challenges due to harsh reaction conditions that might restrict the polymer's suitability for specific substrates, leading to contamination from

* Corresponding author: maria.gomezd@uanl.edu.mx
https://doi.org/10.15251/DJNB.2024.193.1199

leftover reagents. However, chemical vapor deposition offers high-purity films and the capability to regulate coating layers. Nevertheless, the challenges of relying on costly, intricate equipment and the limited suitability for certain substrates that can endure the process conditions are evident [17,18]. However, the present research focuses on creating an uncomplicated and reliable technique for making polythiophene/graphene thin films using an electrochemical method. This method allows for control over the film's structure by adjusting factors like thickness and the range of substrates it can be applied to, including flexible ones [19].

2. Experimental procedure

2.1. Graphene oxide (GO) synthesis

Using the Hummers method, graphene oxide was prepared by mixing pure graphite powder with concentrated sulfuric acid. Afterward, $KMnO_4$ was poured into the reaction mixture. The reaction mixture was stirred for 30 min at room temperature and then heated to 35°C for another two hours with constant stirring. Next, distilled water was dropped slowly onto the mixture; external heating maintained a temperature of 100°C for 15 min. In order to remove excess $KMnO_4$, 30% H_2O_2 was added dropwise and left overnight in room temperature. Following synthesis, the filtrate contained none of the starting materials and the obtained residue was washed with both 10% HCl and distilled water.

2.2. Polythiophene (PTh) and PTh/GO electrodeposition

PTh deposition was performed via chronoamperometry using a PGSTAT302N Metrohm Autolab potentiostat. A typical three-electrode electrochemical setup with ITO glass as the working electrode, platinum wire as the counter electrode, and saturated Ag/AgCl as reference electrode was used for all experiments which were executed at room temperature. The solution contained 0.5 M thiophene monomer and 0.1 M tetrabutylammonium hexafluorophosphate (Bu_4NPF_6) dissolved in dried acetonitrile to obtained PTh thin films with a fixed potential of +1.9 V vs Ag/AgCl. To prepare PTh/GO thin films, GO powder was added to the electrochemical cell under the same conditions.

2.3. Characterization techniques

The morphology and size of the GO were determined by field emission scanning electron microscopy (FESEM) using JEOL JSM6701F. The crystalline structure of the samples was measured by X-ray diffraction (XRD) on a Bruker AXS diffractometer with a CuKα X-ray source of wavelength $\lambda = 1.54184^{o}$ in a scan speed of 0.05º/min over a range of diffraction angles from 20º to 90º. All organic samples were measured by attenuated total internal reflection and Fourier transform infrared (ATR-FTIR) spectroscopy in the range 500-4000 cm^{-1} using a Perkin Elmer Spectrum Two spectrophotometer. Electrochemical measurements were conducted on a Metrohm Autolab PGSTAT302N instrument. Optical absorption spectra were recorded using Shimadzu UV-1800 UV-Vis spectrophotometer while fluorescence spectroscopy was measured through Perkin Elmer LS55 fluorescence spectrometer.

3. Results and discussion

3.1. Graphene oxide synthesis

3.1.1 X-Ray diffraction (XRD)

In Figure 1 we can see the XRD patterns of graphite and GO, which demonstrate different degrees of oxidation. The graphite sample exhibits a strong and sharp peak at approximately $2\theta = 26.5^{o}$, corresponding to the (002) reflection plane, and two relatively weak intensity peaks at approximately $2\theta = 44.5^{o}$ and 54.5^{o}, as shown in Figure 1(a). Compared with the graphite sample, the GO sample in Figure 1(b) exhibits a strong peak at a lower diffraction angle at $2\theta = 9.9^{o}$, while the characteristic peak of graphite loses its intensity at $2\theta = 20.4^{o}$. This change was attributed to the interlayer spacing, indicating the presence of oxygen-containing functional groups within the GO structure [20].

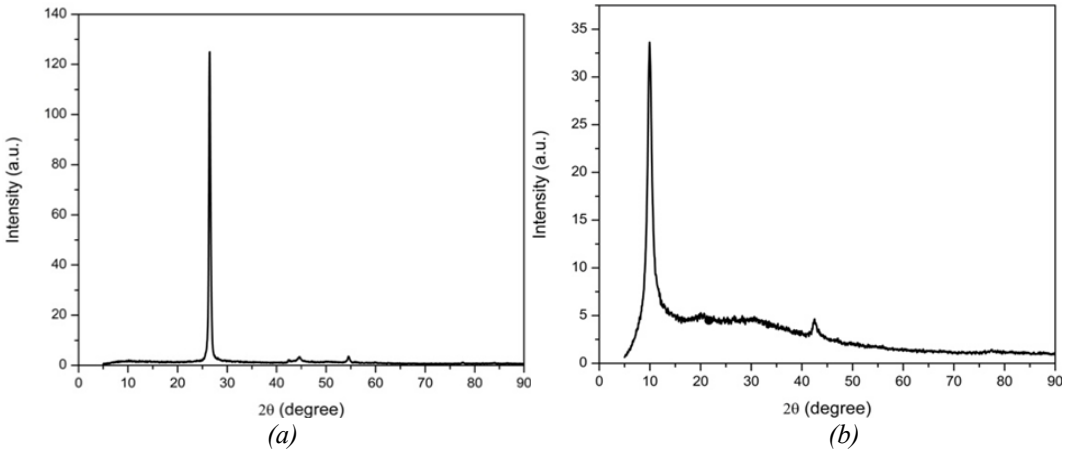

Fig. 1. XRD patterns for graphite(a) and graphene oxide(b).

3.1.2 Fourier transform infrared spectroscopy (FTIR)

Graphite powder and graphene oxide FTIR spectra are presented in Figure 2. Chemical inertness accounts for the absence of a major peak in the FTIR spectrum of pristine graphite. This contrasts with the GO FTIR spectrum having several oxygen-containing functional groups introduced during the oxidation process. The absorption peaks include a very intense band at 3425 cm^{-1} for the O-H stretching vibration of COOH functional groups within its structure. Weaker peaks at 1720 cm^{-1} and 1630 cm^{-1} were assigned to the C=O stretching vibration due to carbonyl, and the C=C stretching vibrations respectively. Additionally, weak bands located at 1400 cm^{-1}, 1228 $cm^{-1,}$ and 1113 cm^{-1} show O-H deformation, C-O stretching vibration of epoxy groups and C-O stretching vibration of alkoxy groups respectively.

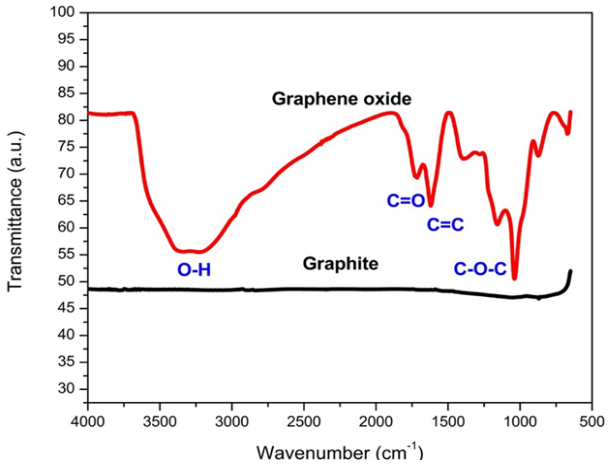

Fig. 2. FTIR spectra of graphite and graphene oxide synthesized.

3.1.3. Field emission scanning electronic microscopy (FESEM)

Figure 3 shows a typical SEM image of GO, which shows a sheet morphology, indicating a good exfoliation process of graphite.

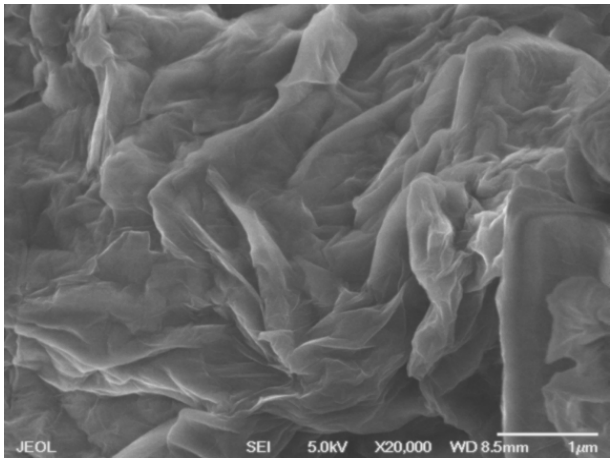

Fig. 2. SEM image of graphene oxide sheets synthesized.

3.2. GO/PTh thin films

3.2.1. Cyclic voltammetry analysis (CV)

The synthesis of polythiophene films begins with the oxidation of the monomer. This step involves subjecting the monomer to an appropriate oxidation potential, which promotes the formation of monomer cations. These cations then concentrate at the surface of the working electrode, leading to the formation of a thin film. Doping and de-doping represent reversible processes that maintain the integrity of the polymer backbone. Nonetheless, under conditions of high potential, conductive polymers experience a mechanism of over-oxidation, a process that is not fully comprehended. This irreversible mechanism leads to accelerated structural degradation and a significant loss of electroactivity [21]. The cyclic voltammograms for thiophene and Bu_4NPF_6 in an acetonitrile solution obtained at 5 mV/s are shown in Figure 4. Voltammogram shows typical electrochemical behavior of PTh with an oxidation peak at +1.3 V associated with a p-doped state, functionalized polymers such as 3-bromo-4-dodecylthiophene exhibits oxidation peaks at +2.4V using the same support electrolyte showing that different reagents (halogenated thiophene monomer) might change the potential window for polymer formation [22]. The obtained thin films exhibit a thickness of 2.03 μm which can be regulated by adjusting the reaction time and/or the concentration of monomer.

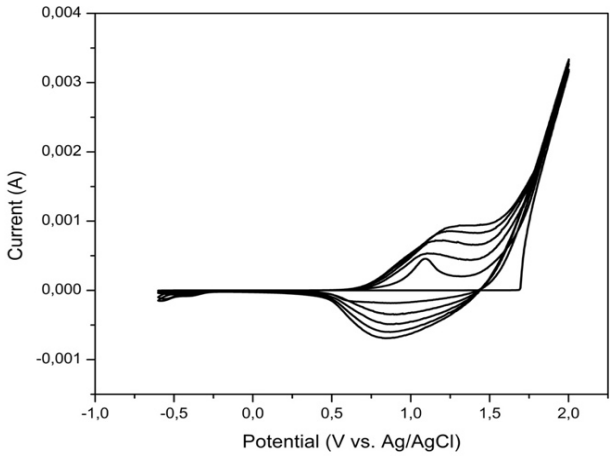

Fig. 4. Cyclic Voltammetry curves of PTh in dried acetonitrile containing 0.1 M Bu_4NPF_6 at a scan rate of 5 mV/s.

3.2.2. Chronoamperometry

Polythiophene and polythiophene/GO thin films were successfully produced via chronoamperometry, conducted under a stable anodic potential of +1.9 V, this increase in the potential needed to synthesize the film could be due to interference because of the presence of other substances (GO) in the electrochemical cell because with lower voltages the film wouldn't form on the substrate. Figure 5 shows the typical behavior of the electrodeposition of PTh/GO, where the initial high current is associated with the oxidation and nucleation of the oligomer chains in the solution near the ITO surface. After nucleation, the current (2.7 mA) remained constant over time, indicating that the oligomer chains reached a molecular weight to precipitate on the electrode surface, forming PTh/GO thin films. The obtained thin films had a thickness of 2.42 μm. The thickness shows time dependence, and with increasing time, the film thickness also increases until monomer depletion and oligomer precipitation are reached.

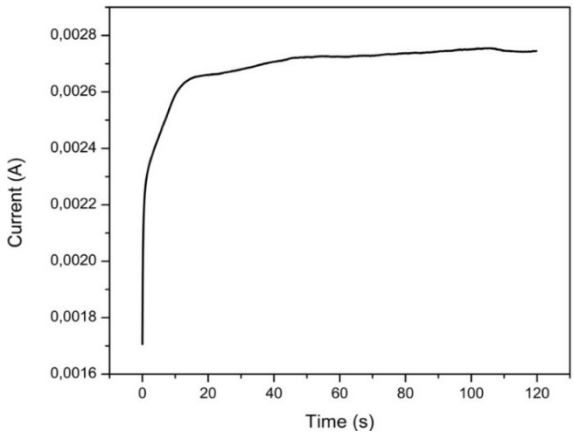

Fig. 5. Chronoamperometry curve of PTh/GO on ITO substrate.

3.2.3. UV-visible analysis

The UV-visible spectrum of PTh/GO thin film is shown in Figure 6. The optical spectrum shows a strong absorption at around 336 nm associated with π–π* transition while the strong absorption at around 485 nm is due to the bipolaron state of the polythiophene[23]. The presence of bipolarons can cause additional absorption peaks in the UV-Vis spectrum that are absent in the spectrum of the neutral (undoped) polymer. The absorption bands of polarons are generally more broad than those observed in neutral species, providing valuable insights into the types of charge carriers present in the material[24].

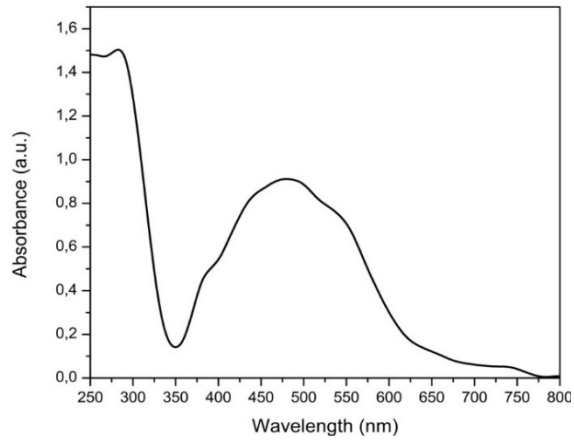

Fig. 6. Absorption spectrum of PTh/GO on ITO substrate.

3.2.4. Photoluminescence analysis (PL)

The PL spectrum of PTh/GO thin film is depicted in Figure 7. Upon excitation at 450 nm, the composite film exhibited three distinct peaks at wavelengths of 496, 536, and 612 nm. These peaks correspond to σ*-n, π–π* and π*-n electronic transitions, respectively. A wider peak indicative of π–π* emission was observed in the composite film associated with the sp^2 carbon atoms derived from both graphene oxide and polythiophene. A conjugated polymer, such as polythiophene, can display redshifts in its absorption peaks, which are influenced by factors such as molecular structure, conjugation length, excitation energy and interactions with other materials. This phenomenon has significant implications for their application in organic electronics and optoelectronic devices[25].

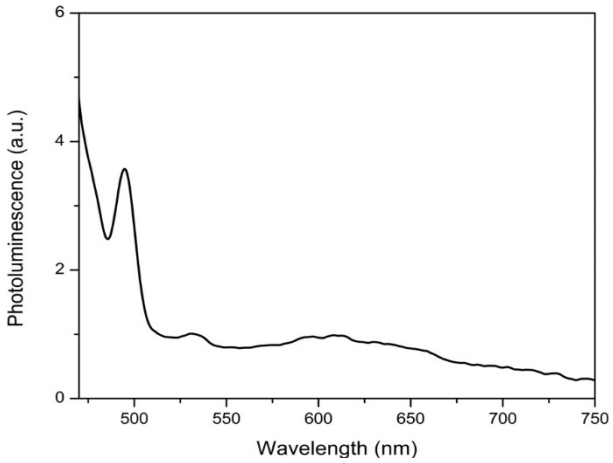

Fig. 7. Emission spectrum of PTh/GO on ITO substrate.

4. Conclusions

This work reports on the electrochemical synthesis of polythiophene/graphene oxide. The graphene oxide was obtained previously using the Hummers method. The bipolaron state of the polythiophene and the π–π* transition in the thin films caused optical absorption at 485 nm and 366 nm. While the emission properties indicate a strong π–π* emission due to sp^2 carbon atoms present in graphene oxide and polythiophene. The effect of the thickness over the electrodeposition time was also investigated.

Acknowledgements

The study was supported by grant 31-BQ-2023 from the PROACTI-UANL. This work was carried out under research program optoelectronic materials of Chemical Sciences Faculty at Nuevo León University. Author José Martínez was supported by CONAHCYT scholarship.

References

[1] Chen Y, Fu K, Zhu S, Luo W, Wang Y, Li Y, et al. Nano Lett 2016;16:3616-23; https://doi.org/10.1021/acs.nanolett.6b00743

[2] Zhan X, Hu G, Wagberg T, Zhan S, Xu H, Zhou P., Microchim Acta 2016;183:723-9; https://doi.org/10.1007/s00604-015-1718-y
[3] Formica N, Mantilla-Perez P, Ghosh DS, Janner D, Chen TL, Huang M, et al., ACS Appl Mater Interfaces 2015;7:4541-8; https://doi.org/10.1021/am5071909
[4] Chunfang F. Stretchable Graphene-based Materials of High Conductivity. Deakin University, 2016.
[5] Zhou Y, Dai D, Gao Y, Zhang Z, Sun N, Tan H, et al., ChemNanoMat 2021;7:982-97; https://doi.org/10.1002/cnma.202100198
[6] Govindaraj P, Mirabedini A, Jin X, Antiohos D, Salim N, Aitchison P, et al., J Mater Sci Technol 2023;155:10-32; https://doi.org/10.1016/j.jmst.2023.01.011
[7] Bosque A del, Sánchez-Romate XF, Sánchez M, Ureña A. Carbon N Y 2022;192:234-48; https://doi.org/10.1016/j.carbon.2022.02.043
[8] Curulli A., Molecules 2023;28; https://doi.org/10.3390/molecules28093777
[9] Zhang L, Guo W, Lv C, Liu X, Yang M, Guo M, et al., Adv Sens Energy Mater 2023;2:100081; https://doi.org/10.1016/j.asems.2023.100081
[10] Kilic NM, Singh S, Keles G, Cinti S, Kurbanoglu S, Odaci D., Biosens 2023, Vol 13, Page 622 2023;13:622; https://doi.org/10.3390/bios13060622
[11] Kim H, Jang JI, Kim HH, Lee GW, Lim JA, Han JT, et al., ACS Appl Mater Interfaces 2016;8:3193-9; https://doi.org/10.1021/acsami.5b10704
[12] Novoselov KS, Fal'Ko VI, Colombo L, Gellert PR, Schwab MG, Kim K., Nature 2012;490:192-200; https://doi.org/10.1038/nature11458
[13] Tanabe I, Ryoki T, Ozaki Y., RSC Adv 2015;5:13648-52; https://doi.org/10.1039/C4RA12503G
[14] Miao J, Fan T., Carbon N Y 2023;202:495-527; https://doi.org/10.1016/j.carbon.2022.11.018
[15] Shindalkar SS, Reddy M, Singh R, Nainar MAM, Kandasubramanian B., Synth Met 2023;299:117467; https://doi.org/10.1016/j.synthmet.2023.117467
[16] Abbasi R, Shineh G, Mobaraki M, Doughty S, Tayebi L., J Nanoparticle Res 2023 253 2023;25:1-35; https://doi.org/10.1007/s11051-023-05690-w
[17] Thanasamy D, Jesuraj D, Konda kannan SK, Avadhanam V., Polymer (Guildf) 2019;175:32-40; https://doi.org/10.1016/j.polymer.2019.03.042
[18] Dianatdar A, Bose RK., J Mater Chem C 2023;11:11776-802; https://doi.org/10.1039/D3TC01614E
[19] Husain A, Ahmad S, Mohammad F., JESC) J Eng 2020;01:36-53.
[20] Liu T, Liu X, Graham N, Yu W, Sun K., J Memb Sci 2020;593:117431; https://doi.org/10.1016/j.memsci.2019.117431
[21] Oberhaus F V., Frense D., Electrochim Acta 2022;402:139536; https://doi.org/10.1016/j.electacta.2021.139536
[22] Goto H, Ochiai B, Matsumura Y. A., Electrochemistry 2023:23-67008; https://doi.org/10.5796/electrochemistry.23-67008
[23] Tsai HW, Hsueh KL, Chen MH, Hong CW., Cryst 2021, Vol 11, Page 1292 2021;11:1292; https://doi.org/10.3390/cryst11111292
[24] Furukawa Y, Shimokawa D., Bull Chem Soc Jpn 2023;96:1243-51; https://doi.org/10.1246/bcsj.20230175
[25] Schö Tz K, Panzer F, Sommer M, Bä H, Kö A., Mater Horiz 2023;10:5538; https://doi.org/10.1039/D3MH01262J